Iranian Journal of Materials Forming 12 (3) (2025) 4-19

Online ISSN: 2383-0042

IJMF

Iranian Journal of Materials Forming

Journal Homepage: http://ijmf.shirazu.ac.ir

Research Article

Predicting Maximum Process Temperature in Cortical Bone Milling: An XGBoost Approach with Sensitivity Insights

V. Tahmasbi, M. Qasemi and A.H. Rabiee*

Department of Mechanical Engineering, Arak University of Technology, Arak, Iran

ARTICLE INFO

Article history:

Received 30 March 2025
Reviewed 17 May 2025
Revised 27 May 2025
Accepted 10 June 2025

Keywords:

Bone milling
Process temperature
XGBoost
Optimization
Biomedical engineering

Please cite this article as:

Tahmasbi, V., Qasemi, M., & Rabiee, A. H. (2025). Predicting maximum process temperature in cortical bone milling: an XGBoost approach with sensitivity insights. *Iranian Journal of Materials Forming*, *12*(3), 4-19. https://doi.org/10.22099/IJMF.2025.52838.1330

ABSTRACT

Bone milling, a crucial biomechanical process in medical engineering, finds applications in dentistry, orthopedic surgery, and bone-related treatments. The utilization of computer numerical control (CNC) surgical mills has significantly enhanced this process, but it comes with challenges such as elevated temperatures that induce thermal necrosis in bone tissue. This study examines key inputs, including tool diameter, feed rate, rotational speed, and cutting depth, conducting a detailed experiment to predict maximum process temperature using the XGBoost machine learning algorithm. The XGBoost model consistently demonstrated exceptional predictive accuracy, yielding high determination coefficients of 0.99 in training and 0.94 in testing. Accurate predictions were evident through close alignment between model-predicted and actual values, with mean absolute percentage error (MAPE) values of 0.33% and 3.38% for training and testing, respectively. Rotational speed emerged as a critical factor, indicating a key point where temperature trends shift. Higher speeds are correlated with lower temperatures due to enhanced chip removal and reduced bone heat conductivity. Elevated feed rates were associated with increased bone temperature, emphasizing the intricate interplay between frictional forces and heat production. Additionally, often-overlooked factors like cutting depth and tool diameter substantially influenced process temperature, impacting surgery recovery times. Sobol sensitivity analysis identified cutting depth, rotational speed, tool diameter, and feed rate as primary factors influencing maximum process temperature fluctuations, with effectiveness percentages of 46.7%, 36%, 13.2%, and 4.1%, respectively. This comprehensive analysis sheds light on optimizing bone milling processes and mitigating thermal risks in medical applications.

1. Introduction

Most orthopedic surgeries involve bone cutting and/or machining, with the machining process including grinding, sawing, drilling, milling, and turning [1, 2]. Sport injuries, aging and high-weight overloads are major causes of orthopedic issues, leading to the increasing prevalence of total knee arthroplasty (TKA) [3]. This surgery is necessary due to knee abrasion. The common method to prepare the surface for an artificial joint is bone sawing, which can result in high temperature and rough surfaces [4, 5]. Milling, on the

* Corresponding author
E-mail address: rabiee@arakut.ac.ir (A.H Rabiee)
https://doi.org/10.22099/IJMF.2025.52838.1330

other hand, is employed to produce more accurate surfaces. Accurate orientation and positioning of the bone during femur and tibia surgeries are crucial for the proper functioning of the ligaments and the knee [6]. When assisted by robots, milling can achieve higher resilience and accuracy [7]. Bone surgery is frequently performed in cranial, otological, and spinal operations [8]. Force and temperature play crucial roles in bone machining. Excessive heat can lead to increased tissue damage and potential breakage which in turn can cause infection and thermal necrosis (cell death) [9]. In knee replacement, the occurrence of thermal necrosis can impair bone development around the prosthetic joint [10]. Thermal necrosis disrupts blood flow, degrades tissue, and compromises bone integrity [11]. The extent of the bone injury depends on the temperature and the duration of contact [12]. Various studies indicate that thermal necrosis is more likely to occur within the temperature range of 44 to 100 °C, with temperatures above 70 °C resulting in acute thermal necrosis. In a study on rabbit bone, Berman et al. [13] found that thermal necrosis became inevitable once the temperature reached 70 °C. Lundskog [14] in his studies of rabbit bone concluded that bone temperature of 55 °C for 30 seconds leads to inevitable cell death. Bonfield and Li [15] observed similar effects in dog's femur, with thermal necrosis occurring at 55 °C. Eriksson et al. [16], through microscopic examination of rabbit bone, found that maintaining bone temperature of 47 °C for one-minute results in thermal necrosis. In a follow up study, they noted that increasing the temperature from 47 to 50 °C had a detrimental effect on bone, while temperatures below 44 °C did not cause harm within one minute [17]. It should be mentioned that these reports focused on animal bones, which may differ from human femurs. The precise behavior of thermal necrosis in human bones is still not fully understood. Researchers propose that temperatures above 47 °C for one minute could lead to thermal necrosis in human bones [18].

Therefore, optimizing the process temperature is essential for a successful operation, Al-Abdullah et al. [19] investigated cancellous bone machining and predicted the process temperature based on experimental rotational speeds and feed rates. Liao et al. [20] employed an analytical method to calculate the temperature variation in the bone's cutting area. The most and least optimal cutting orientations were found to be 60 and 30 degrees, respectively, according to Esteon's direction. Tahmasbi et al. [21] employed the response surface method (RSM) to model the process temperature in bone drilling, focusing on the impact of input parameters on temperature. They found that the temperature increased in correlation with the rotational speed, whereas the impact of feed rate was more intricate as indicated by the reference. Hassanalideh and Gholampour [22] examined the impact of tool diameter, drilling depth, and drilling angles on temperature and compared their experimental findings with results from the finite element method. They found that increase in drilling depth and bit diameter, along with a reduction in drilling angles, led to higher temperatures. Shin and Yoon [23] developed an analytical heat model to predict bone temperature distribution during milling. They utilized thermal imaging cameras to capture the temperature of the freshly milled surface. The highest temperature ranged from 49 and 115 °C, with thermal necrosis expected to occur at a depth of 2 mm. Increasing feed rates and reducing cutting depths were found to lower the maximum temperature. Sugita et al. [24] explored the temperature distribution in pig bone during grinding. They determined the temperature distribution using a linear movable heat source on an infinitely long surface. Thermocouples measured the tool's temperature, while a thermograph assessed the bone's temperature. The model and experimental results confirmed the potential for heat necrosis within 0.1 millimeters of the surface. Their research showed that cutting temperature increased with the feed rate. Malvisi et al. [25] recorded the highest temperature fluctuations during grinding and sawing procedure and evaluated various tools to reduce the temperature.

Applying machine learning techniques to predict temperatures in machining operations is a crucial area for enhancing the efficiency and precision of these processes. Machine learning algorithms can significantly enhance temperature prediction due to the

intricate and varied working conditions. These techniques can identify patterns and intricate connections among variables, thereby enhancing precision in determining process parameters [26-28]. By utilizing machine learning techniques and artificial intelligence, it is possible to reduce energy wastage, extend tool lifespan, and improve productivity in machining operations. Recently, there has been a substantial focus on utilizing various machine learning techniques to predict temperature, tool life, surface roughness, tool wear, and cutting force during milling operations. For instance, Liu et al. [29] extensively analyzed remaining features, such as full-width half-maximum and stress of the ball screw raceway following dry machining. They used machine learning methods like neural networks and support vector machine (SVM). SVM outperformed neural networks in predicting machining parameters and improving ball screw performance. Du et al. [30] analyzed quality parameters in CNC machining with a specific focus on cutting force and spindle vibration as the variables. A power spectrum-based feature extraction method was suggested, which achieved good prediction accuracy using neural network. The coefficient of determination was 0.92 for roughness, 0.86 for profile, and 0.95 for roundness. He et al. [31] utilized a deep learning approach, namely the stacked sparse autoencoders model with a backpropagation neural network, to predict tool wear by examining raw temperature data from an intelligent cutting tool. The methodology surpassed conventional approaches, demonstrating superior accuracy and reliability in forecasting tool wear. Varghese et al. [32] studied tool condition monitoring in micro-milling to forecast tool life phases until breaking by analyzing force data. The study utilized the random forest machine learning technique and achieved a prediction accuracy of 88.5%, which was exceptional. Adding an initial cutting-edge radius improved the model's performance much further. Tahmasbi and Rabiee [33] investigated temperature forecasting in robotic bone grinding by utilizing the design of experiments and an adaptive neuro-fuzzy inference system (ANFIS) enhanced with the teaching-learning-based optimization algorithm. ANFIS accurately predicted temperatures, with minimal errors of 1.74% during training and 3.17% during testing. Safari et al. [34] explored the concurrent development of force and temperature while drilling bones, focusing on helix and point angles. They utilized a central composite experimental combined with an ANFIS network optimized by particle swarm optimization (PSO). The ANFIS-PSO model accurately forecasted force and temperature, with mean errors of 1.249% and 3.818%, respectively. Their analysis showed that higher helix and point angles reduced temperature but raised force, with helix angle changed having a slightly greater impact. Banda et al. [35] studied optimizing the progression of flank wear width during face milling of Inconel 718, addressing the challenges posed by intricate wear mechanisms. They utilized Gaussian kernel ridge regression to create a model that achieved a root mean square error of 30.9 μm and a determination coefficient of 0.93. This experimentally validated model helps predictand optimize vibration behavior during real face milling operations of Inconel 718. Rabiee et al. [36] investigated the impact of micro-milling parameters on cutting force and temperature during cortical bone operations. By utilizing support vector regression (SVR) and sensitivity analysis, researchers developed a highly accurate SVR predictor. This tool enables surgeons to anticipate and optimize machining conditions, ultimately minimizing temperature and cutting force before surgery. Zeng and Pi [37] employed a hybrid model combining physics-based simulation and machine learning to predict milling forces. This method significantly improved precision, reaching an accuracy of up to 98%, even with limited test data, particularly for various materials and unique milling equipment. Araghizad et al. [38] utilized deep learning to forecast milling surface roughness by combining physical principles with deep learning. Data augmentation and a physically guided loss function were implemented. The convolutional neural network model outperformed current techniques, improving prediction accuracy by an average of 3.029%, showing promising advancements in machine learning.

This study examines how input parameters, such as the tool's rotating speed, feed rate, cutting depth, and diameter, as well as their relationships, impact process temperature during bone milling. Necrosis is a significant issue in orthopedic surgery that can lead to surgical inefficiency. This work investigates the occurrence and non-occurrence of necrosis during bone grinding. Therefore, it is essential to understand the impact of each input parameter and their interactions on the temperature increase in surgeries involving milling instruments. Optimizing milling parameters is crucial to achieve ideal machining conditions and minimize the risk of necrosis. Identifying safe zones where necrosis is unlikely is essential to ensuring safe surgical procedures. These concerns regarding bone grinding remain unresolved. The end milling procedure was conducted vertically on the cortical bone. Various factors, including rotating speed, feed rate, cutting depth, and tool diameter, were used to measure temperature. The XGBoost approach was employed for intelligent modeling, and the Sobol method was used for sensitivity analysis to quantitatively and qualitatively assess the outcomes.

2. XGBoost Machine Learning Model

XGBoost is a highly accurate and efficient machine learning model that can be employed for predicting crucial outcomes in various machining processes. This method utilizes the gradient boosting algorithm and excels at modeling intricate and non-linear interactions [39]. XGBoost is structured as an ensemble model, utilizing a collection of weak models as boosters to create a stronger model. This method uses decision trees as a base model and iteratively enhances the model using an incremental approach. XGBoost stands out for its capability to efficiently handle time and memory, making it well-suited for complicated tasks [40]. This method also incorporates techniques like feature selection and dimension reduction to enhance performance and mitigate overfitting. XGBoost is a versatile approach known for its numerous capabilities, such as customizable hyperparameters. This method involves specifying different hyperparameters, including learning rate, maximum tree depth, number of trees, gamma, etc. These factors significantly impact the model's performance and accuracy. For example, a lower learning rate steadily strengthens the model step by step, potentially resulting in improved accuracy and preventing overfitting. Increasing the maximum depth of the tree can enhance the model's predictive capability. However, this increment must be executed cautiously to prevent overfitting. Moreover, adding more trees can lead to a higher number of models and potentially improve accuracy. However, a significant rise could be linked to issues with time and memory. Increasing the proportion of randomly selected samples compared to the total samples leads to heightened variability in the data, aiding in the prevention of overfitting. Gamma determines the point at which the model is trained to reduce errors. Decreasing this parameter could mitigate overfitting. Based on the mentioned impacts, precise adjustment of hyperparameters is essential to enhance the efficiency of the XGBoost model in forecasting the bone machining temperature. Adjusting these hyperparameters can enhance the XGBoost model's capability to accurately forecast the machining temperature during bone milling. This approach excels at modeling intricate relationships and is adept at identifying various patterns in temperature data during the machining process. The XGBoost model's adaptability has established it as an effective tool for temperature prediction and control in diverse industrial settings [41]. In this study, the XGBoost model was developed and implemented using the Python programming language in the Google Colab environment. XGBoost was chosen over other ensemble and deep learning methods due to its superior performance with small datasets, its effective regularization mechanisms, and its ability to model complex nonlinear relationships with low computational overhead.

3. Sensitivity Analysis

Sensitivity analysis in engineering is a valuable method for assessing the impact of individual variables on a system's overall response. This study can be categorized as deterministic or probabilistic depending on its

approach, or as graphical, mathematical, or statistical depending on its form. The graphical sensitivity analysis method represents sensitivity using diagrams, tables, and surfaces. This method is used when the variation of output is illustrated upon the change in input parameters. Nonetheless, in the mathematical method, the sensitivity is derived mathematically from the variation of the output when input parameters are varied. Computational tools in this method can sense the variation in the output even with an infinitesimal change in input parameters. Finally, in the statistical sensitivity analysis method, simulation of input variables as probabilistic distributions is performed. Subsequently, the impact of these input parameters is assessed on the system's output. These methods allow for the simultaneous evaluation of the impact of certain input factors.

Sobol sensitivity analysis is a statistical tool for sensitivity analysis that is model-independent and relies on variance decomposition. This technique is suitable for non-linear and non-uniform systems [42]. The Sobol method was selected for sensitivity analysis due to its ability to provide a detailed and reliable quantitative assessment of both the direct and interaction effects of input parameters on the model output. Unlike qualitative screening methods such as Morris, which only offer approximate rankings of input importance, or ANOVA-based methods that rely on assumptions like linearity, the Sobol method is model-independent and capable of decomposing the variance of the output into contributions from each input and their interactions. Despite its higher computational cost, this approach is particularly suitable for complex models like ours, where multiple input parameters (tool diameter, feed rate, rotational speed, and cutting depth) can interact in non-trivial ways to influence the maximum process temperature.

Sobol sensitivity analysis is a statistical tool for sensitivity analysis that is model-independent and relies on variance decomposition. This technique is suitable for non-linear and non-uniform systems [43]. The model is represented by the equation Y = f(X), where Y is the output of the model and X is a vector containing input parameters $x_1, x_2, \dots, x_n$. The variance of the model output V is calculated by summing the variances of each decomposed term as shown in Eq. (1):

$$V(Y) = \sum_{i=1}^{n} V_i + \sum_{i \le j \le n}^{n} V_{ij} + \cdots + V_{1,\dots,n} \quad (1)$$

The term V_i represents the first-order impact of each input parameter, whereas V_{ij} is the interaction effect among n factors, calculated as $V\left[E\left(Y|x_i, x_j\right)\right] - V_i - V_j$.

Sensitivity indices are expressed as the ratio of the variance of a specific order to the total variance. For example, $S_i = V_i/V$ represents the first-order sensitivity index, and $S_{ij} = V_{ij}/V$ represents the second-order sensitivity index, and so on.

The total sensitivity index, which represents the overall impact of each parameter, is calculated by summing all orders of sensitivity indices as shown in Eq. (2):

$$S_{Ti} = S_i + \sum_{i \neq j} S_{ij} + \cdots \quad (2)$$

Complementary explanations and details about the Sobol method can be found in [44]. To determine an appropriate sample size for Sobol sensitivity analysis, a convergence test was conducted by gradually increasing the sample size from 100 to 5000. The evolution of both first-order and total-order indices was monitored as a function of sample size. The indices showed noticeable variations up to around 1000 samples, but remained stable beyond that point. Although further increasing the sample size led to more scattering and longer computation times, no significant improvements in the stability or accuracy of the indices were observed. Therefore, a sample size of approximately 1000 was chosen to ensure a balance between computational efficiency and result reliability.

4. Experimental Procedures

4.1. Material and limitation

Bovine cortical bone is commonly used as a model for human cortical bone in biomechanical and thermal studies due to its availability and similar structural characteristics. The physical and mechanical properties

of bovine cortical bone are close to those of human long bones. Therefore, many researchers have used the bovine femur to investigate the cortical bone drilling process. Table 1 shows some physical and mechanical properties of fresh bovine cortical bone and fresh human cortical bone. Both bones are composed largely of hydroxyapatite and collagen, giving them comparable stiffness and strength. Thermal properties are quite close, as both are largely mineralized tissues. Variability in microstructure (e.g., Haversian system density) can influence crack propagation and fatigue properties. Slight differences may arise due to age, disease state, or gender. With appropriate modeling and safety adjustments, bovine-based findings can be a strong foundation for developing human clinical protocols.

Table 1. Comparison for the properties of human cortical bone and bovine cortical bone

Bone property	Human	Bovine
Tensile strength (MPa)	140-250	130-200
Compressive strength (MPa)	45-150	40-145
Young's modulus (GPa)	10-22	10-17
Shear modulus (MPa)	3	3
Density (kg/m^3)	1950-2100	1800-2000
Poisson's ratio	0.33	0.4
Specific heat (J/kg.K)	1300	1330
Thermal conductivity (W/m.K)	0.1-0.3	0.1-0.43

4.2. Method

The design of experiments (DOE) approach plays a crucial role in optimizing the bone milling process by enabling systematic and structured testing of influential parameters. This methodology allows for the identification of key variables and facilitates the determination of optimal conditions to achieve accurate and reliable results. By analyzing the influence of each input factor, DOE supports the development of predictive models that clarify interdependencies and improve forecasting accuracy. In this study, maximum bone temperature was selected as the output variable, influenced by input parameters including tool diameter, feed rate, rotational speed, and cutting depth. Five fresh bovine femur samples were selected for experimentation, focusing on the diaphysis region, approximately 90 cm in length, composed of cortical bone with a thickness ranging from 8 to 10 mm. Table 2 provides the physical characteristics of each bone sample. To prepare the samples, both ends of the bones were trimmed using a saw. To enhance the reliability of the results, each experimental condition was repeated three times, and the average of the maximum temperature values was recorded. The use of DOE in this context enhances process efficiency, reduces material waste, and promotes improved clinical outcomes. Fig. 1 illustrates the experimental setup, and Table 3 presents the outcomes of all 27 experimental conditions. It is worth noting that these experimental procedures and results were previously reported in [33]. For the sake of brevity, detailed descriptions are omitted here, and readers are encouraged to refer to the cited work for additional information.

5. Results and Discussion

5.1. Temperature modeling

The XGBoost machine learning algorithm was utilized to develop the model based on the outcomes of experiments. The hyperparameter values significantly impact the accuracy and robustness of the model. The hyperparameters for learning rate, maximum tree depth, number of trees, and gamma are set to 0.1, 6, 1000, and 0, respectively. In this study, hyperparameter values such as learning rate, maximum tree depth, number of trees, and gamma were determined through a series of

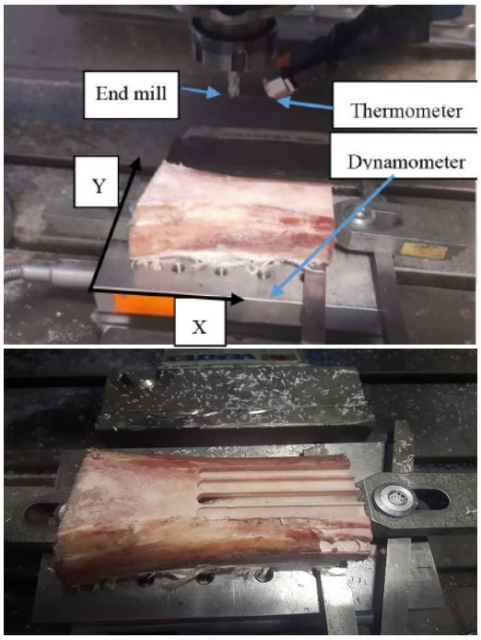

Fig. 1. Experimentation tooling and setup in study of bone milling.

Table 2. Bone specification used for milling

Sample	Age (year)	Sex of bovine	Slaughter time	Min. of sample width	Sample length	Max. of thickness
1	3	bull	3h	40 mm	9 cm	1 cm
2	3-3.5	bull	4h	45 mm	10 cm	1.5 cm
3	3-4	bull	3.5h	38 mm	8.5 cm	1 cm
4	4	bull	4.5h	42 mm	9.5 cm	1.2 cm
5	3.5	bull	3h	45 mm	10.5 cm	1.5 cm

Table 3. Experimental findings on temperature variations dependent on bone milling input parameters [33]

Set number	N (rpm)	F (mm/min)	Depth (mm)	D (mm)	T (°C)
1	1000	100	1	4	42.3
2	3000	100	1	4	50.4
3	1000	300	1	4	48
4	3000	300	1	4	46.8
5	1000	100	3	4	58.7
6	3000	100	3	4	68.1
7	1000	300	3	4	62.5
8	3000	300	3	4	65.4
9	1000	100	1	8	52.3
10	3000	100	1	8	55.3
11	1000	300	1	8	58.8
12	3000	300	1	8	54.4
13	1000	100	3	8	63.5
14	3000	100	3	8	72.2
15	1000	300	3	8	65.4
16	3000	300	3	8	64.7
17	1000	200	2	6	57.5
18	3000	200	2	6	65.1
19	2000	100	2	6	66.2
20	2000	300	2	6	69.8
21	2000	200	1	6	64.4
22	2000	200	3	6	74.5
23	2000	200	2	4	59.6
24	2000	200	2	8	67.3
25	2000	200	2	6	70.1
26	2000	200	2	6	69.8
27	2000	200	2	6	68.7

manual tests. XGBoost's robustness allowed the model to perform well across a broad range of parameter values, reducing the sensitivity to exact tuning. To assess and mitigate overfitting, the model's performance was evaluated on a separate test dataset that was not involved in the training process.

Fig. 2 displays a scatter plot used for predicting the temperature of the milling process in two separate phases: training and testing. The graphic displays actual values in relation to predicted ones using XGBoost, with green and orange symbols denoting training and test data, respectively. The middle line A = P is provided for better accuracy assessment of the model. The training data aligns with the middle line. To evaluate the model's accuracy, it is essential to focus on the test data as it was not utilized during the development of the model. The data from the test section closely align with the middle line, indicating the excellent effectiveness of the XGBoost model.

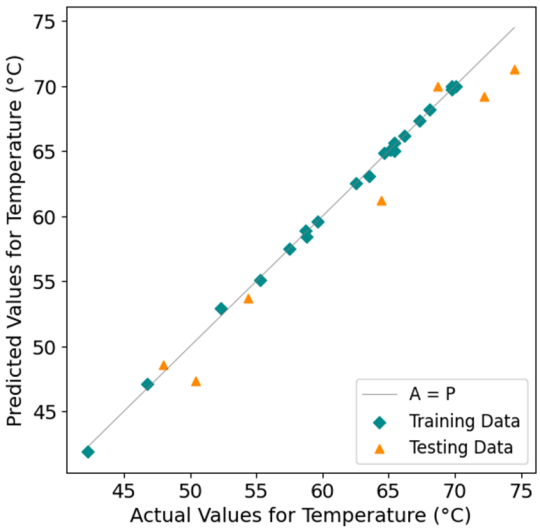

Fig. 2. Actual data in terms of predicted ones by XGBoost in two parts of training and testing.

Fig. 3 displays the temperature of the process for all samples, comparing predicted and actual data in two phases: training and testing. The predicted data during the training phase (blue symbols) align with the actual data in this phase (green solid line). It is evident that the predicted results during the test phase closely match the actual data. The model's accuracy is higher in the training phase than in the testing stage due to the utilization of training data in the learning process, while the test data is set aside for accuracy assessment.

Fig. 4 displays a histogram illustrating the error between the predicted and actual data for the process temperature in two phases: training and testing. The error formation is predominantly centered around zero during the training phase. During the training phase, the error values typically fall within the range of -0.6 to 0.4. In contrast, during the testing phase, the error values are observed to be within the range of -1 to 3.

The XGBoost model is quantitatively evaluated using root mean square error (RMSE), mean absolute error (MAE), determination coefficient (R^2), and mean absolute percentage error (MAPE), for both the training and testing stages, as shown in Table 4. The RMSE and MAE values for the training data are exceptionally low and near zero. It is essential to focus on the error criteria in the test stage to evaluate the efficiency of the model, which is also low. MAPE and R^2 are superior measures for comparing machine learning models. MAPE is 0.33% for the training phase and 3.38% for the testing stage. The coefficients of determination for the training and testing phases are computed as 0.99 and 0.94, respectively, indicating the great accuracy of the XGBoost model in predicting the process temperature in this study.

Table 4. MAE, RMSE, MAPE and R^2 for predicting temperature in both the training and test phases

	MAE	RMSE	MAPE (%)	R^2
Train	0.19	0.25	0.33	0.99
Test	2.13	2.41	3.38	0.94

5.2. Effect of input parameters

This section analyzes the impact of feed rate, rotational speed, tool diameter, and cutting depth on process temperature using the XGBoost machine learning model with an expanded dataset. The Sobol approach enables the simultaneous adjustment of all parameters, unlike graphical methods, which typically alter one variable at a time while keeping others constant. Up to now, there is no exact report value in which thermal necrosis of human bone would occur. However, temperature as high as 47 °C, is considered sufficient to initiate thermal necrosis in human bone. An increase of just 5 °C to 52 °C can causes thermal necrosis within 1 minute. However, this threshold applies more to bone drilling, where the tool remains stationary for a longer period. In bone milling, the tool rapidly removes chips and moves away, with higher feed rates causing the tool to move further away more rapidly. The relatively low thermal conductivity and specific heat of bone lead to quicker heat distribution, making the threshold of 47 °C less appropriate for bone milling. On the other end of spectrum, at higher temperatures of 70 °C, thermal necrosis becomes abrupt and inevitable. Given the nature of the milling process, where the tool quickly moves away from the cutting zone, a triggering temperature of 55 °C is considered for the initiation of thermal necrosis. While previous studies have often cited 44 °C as the threshold for thermal necrosis, more recent findings suggest that temperatures up to 55 °C for durations under 30 seconds do not cause irreversible bone damage. Given the transient nature of heat in bone milling, where the tool moves continuously and the heat dissipates quickly, 55 °C is considered a clinically reasonable limit. This selection aligns with reported clinical observations and allows for more flexibility in optimizing machining parameters without compromising patient safety.

The temperature response surface based on tool diameter, feed rate, rotational speed, and cutting depth is depicted in Fig. 5. Fig. 6 shows interaction effects of feed rate and rotational speed at different cutting depths, while Fig. 7- 10 illustrate temperature evolution with the main input parameters. The data points in these graphs were generated using SimLab software with the Sobol method. From this point onward, the temperature unit in all figures is expressed in degrees Celsius.

As depicted in Fig. 5, The process temperature is significantly influenced by rotational speed and feed rate

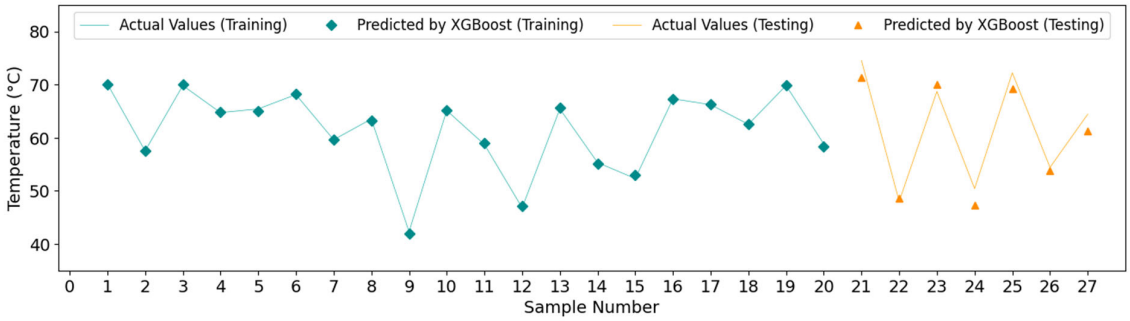

Fig. 3. Process temperature for all samples for predicted and actual data in two stages of training and testing.

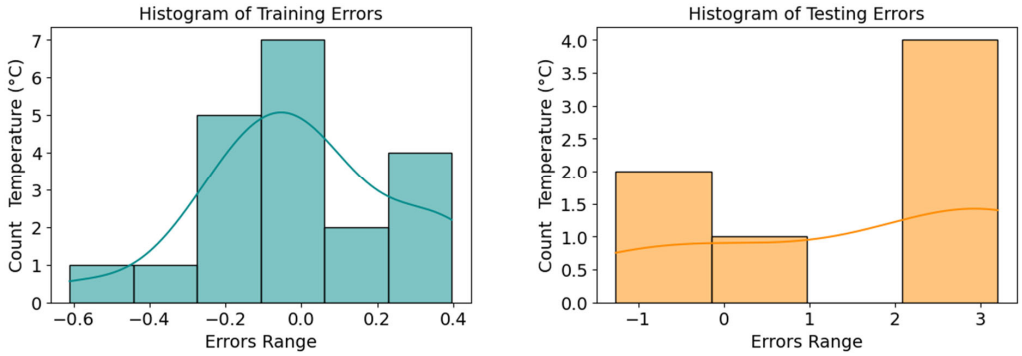

Fig. 4. The discrepancy between the predicted and actual data during the training and testing stages.

with a saddle point exhibiting a maximum along the rotational speed axis and a minimum along the feed rate axis. This critical point is crucial, as previous reports have suggested lower temperatures with lower rotational speeds or higher speeds. As illustrated in Fig. 7, when the rotational speed increases, the temperature first grows until reaching a critical point, then drops. Lower rotating speeds result in minimal bone injury, and it is possible to reach temperatures below 47 °C with high-speed milling. This is due to reduced process forces caused by easy chip removal from the machined groove, which is attributed to the bone's weaker thermal conductivity compared to the tools. The results indicate that high-speed milling decreases thermal necrosis by reducing the rate of temperature increase at higher cutting speeds.

Feed rate is a crucial factor in the selection of a tool type and feed rate, as it affects the velocity of the heat source. The thermometer's accuracy and precision, along with the chosen tool type and feed rate range, significantly influence the selection of feed rate. The study uses a thermometer to measure the temperature at the point where the tool meets the freshly machined bone surface. The study shows that bone temperature typically increases with a rise in feed rate as illustrated in Fig. 8. At smaller feed rates, the process force, tool-bone friction, and cut chip thickness are reduced, leading to lower heat generation and temperature levels. However, at high feed rates, the force applied to the workpiece and chip thickness increases exponentially, resulting in increased heat generation. Larger feed rates generally result in higher temperatures within the investigated range of input variables.

Cutting depth has been largely overlooked in previous studies, with only one study by Shin and Yoon [23] exploring its impact at a cutting depth of less than 1 mm. The study found that increasing cutting depth led to higher process temperatures, as depicted in Fig. 9. Other studies have typically assumed a constant cutting depth. However, cutting depth significantly influences the material removal rate and the duration of surgery. This paper investigates cutting depths ranging from 1 to 3 mm, showing that increasing cutting depth results in higher process temperatures due to the larger contact area, which requires more force to detach the chip from the base, leading to increased friction, forces, and heat production.

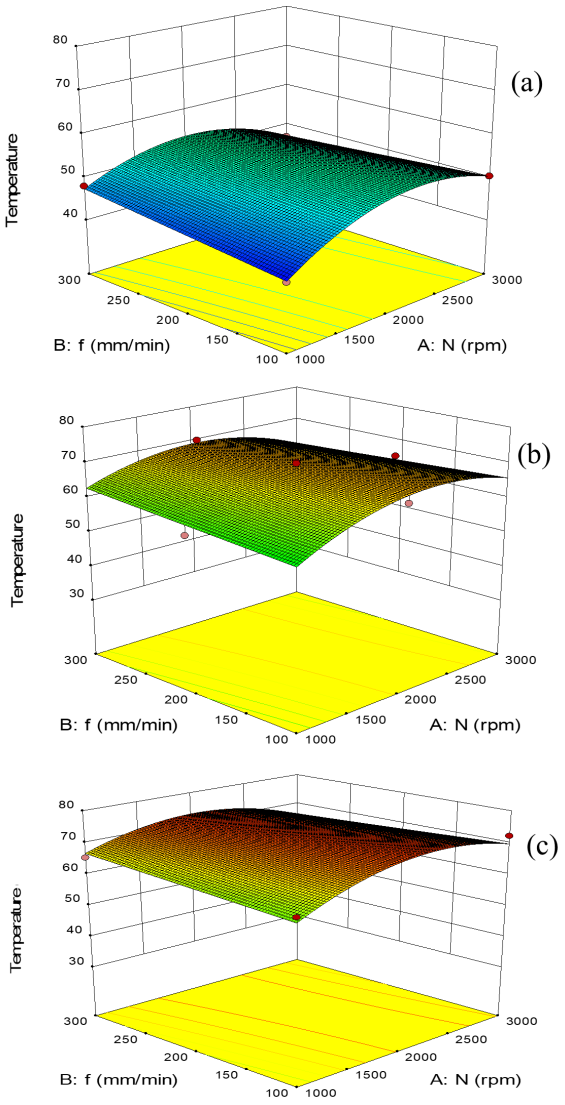

Fig. 5. Temperature response surface based on rotational speed (N) and feed rate (f) at different cutting depths with tool diameters (D) of 4 mm: (a) cutting depth = 1 mm, (b) cutting depth = 2 mm, and (c) cutting depth = 3 mm.

The tool diameter plays a crucial role in generating heat and thermal necrosis during a process. Fig. 10 illustrates that larger tool diameters result in increased temperatures due to the extended contact area, in which leads to higher heat and frictional forces. Larger diameters also increase axial force, positively impacting heat production. Overall, temperature rises exponentially with increasing tool diameter. For instance, a tool with an 8 mm diameter has a narrower safe zone for thermal necrosis compared to 6 mm or 4 mm diameters. In medical terms, using a thinner tool diameter can reduce the surgery's recovery period.

5.3. Sensitivity analysis

Based on the diagrams shown in Fig. 7-10, it can be deduced that cutting depth, rotating speed, tool diameter, and feed rate have the most significant impact on the maximum process temperature within the range of input parameters analyzed. This can be computed considering the slope of graphical representation of each diagram. Sobol sensitivity analysis offers advantages over analysis of variance (ANOVA) in several aspects. In addition to providing a qualitative understanding, it can

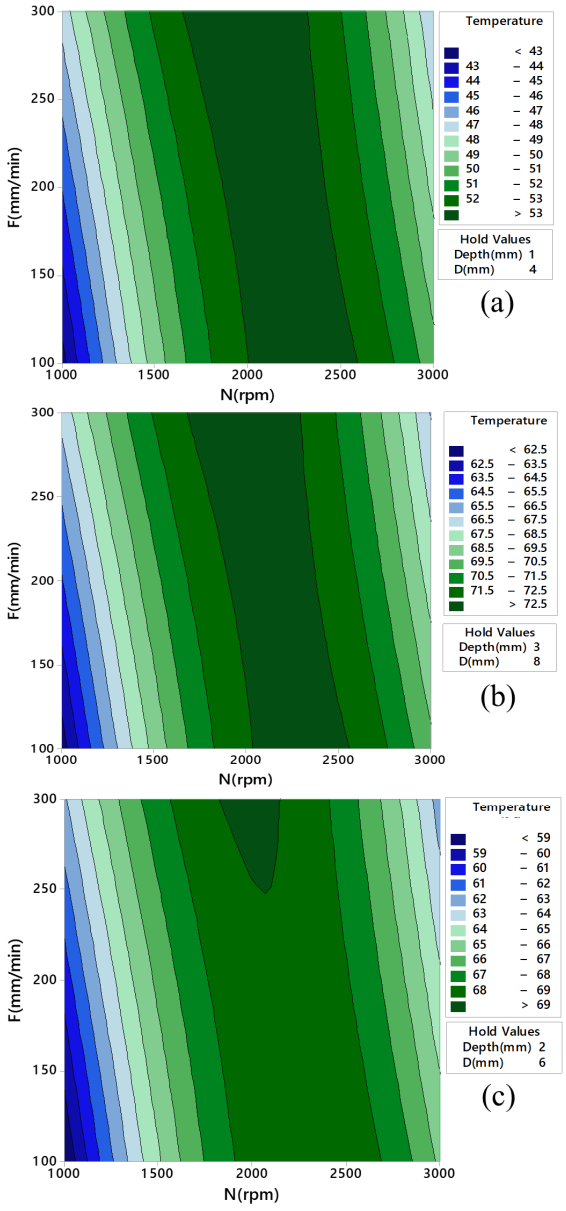

Fig. 6. Interaction effects of feed rate (f) and rotational speed (N) in different cutting depths and tool diameters on process temperature: (a) cutting depths: 1 mm, tool diameter: 4 mm, (b) cutting depths: 3 mm, tool diameter: 8 mm, and (c) cutting depth: 2 mm, tool diameter: 6 mm.

simultaneously identify all the effective parameters. However, when analyzing the interaction effects of parameters, the response surface method generally yields more reliable results than Sobol sensitivity analysis.

Fig. 11 displays the outcomes of Sobol sensitivity analysis. The Figure indicates that cutting depth has the most significant effect at 47.7%, followed by tool rotational speed at 36%, tool diameter at 13.2%, and feed rate at 4.1% on the maximum process temperature.

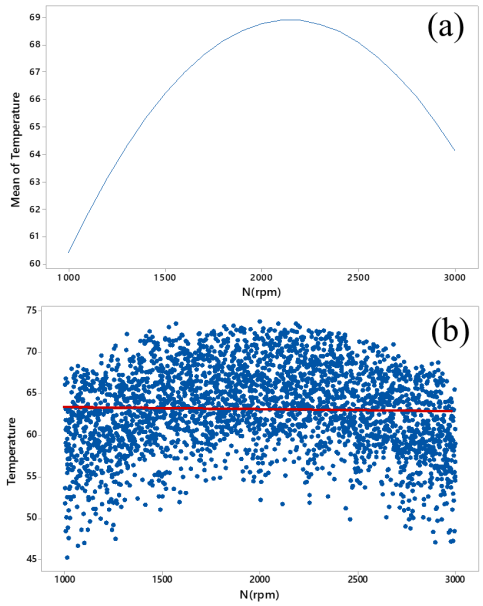

Fig. 7. Impact of rotational speed on temperature: (a) RSM and (b) sensitivity analysis.

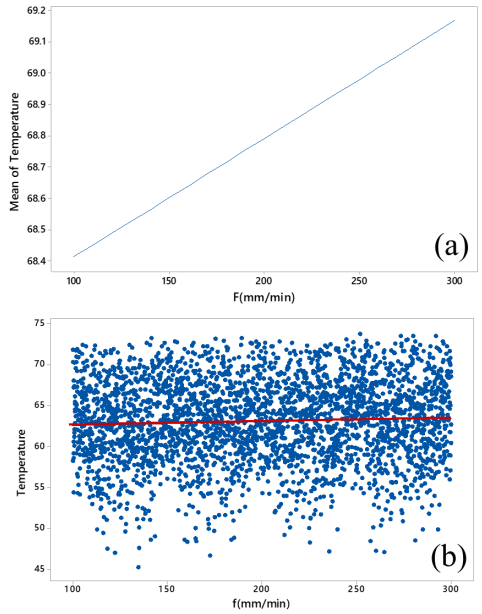

Fig. 8. Impact of feed rate on temperature: (a) RSM and (b) sensitivity analysis.

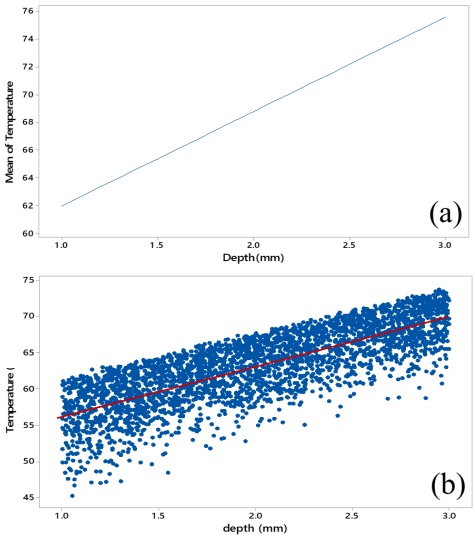

Fig. 9. Impact of cutting depth on temperature: (a) RSM and (b) sensitivity analysis.

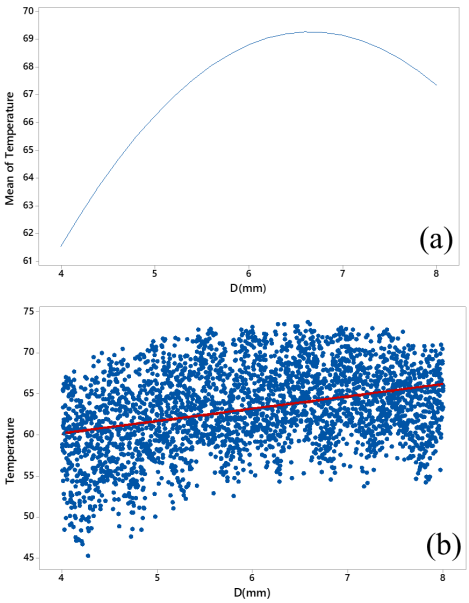

Fig. 10. Impact of tool diameter on temperature: (a) RSM and (b) sensitivity analysis.

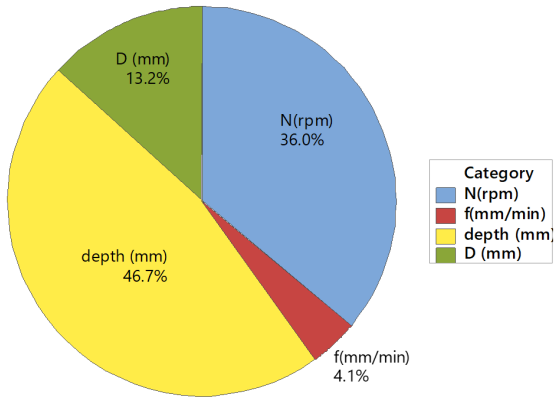

Fig. 11. Effectiveness of each process parameters on process temperature.

5.4. Optimization of process parameters

Optimization of input parameters was performed to find the least maximum process temperature. The optimization was carried out on the proposed model over the range of input parameters. Results are depicted in Fig. 12. To evaluate the prediction of the optimum combination found by the model, validating experimentations were conducted. The results are compared in Table 5.

As can be seen from Table 5, the error of the model in predicting temperature with the optimum combination of input parameters is only 0.28%, which proves the accurate anticipation of the model and its functionality. Thus, the least maximum process temperature occurs with a tool diameter of 4 mm, feed rate of 100 mm/min, rotational speed of 1000 rpm and cutting depth of 1 mm. This temperature is about 42 °C. The diagrams presented in Fig. 12 allow the surgeon to identify the effect of each individual parameter and adjust the input parameters to achieve no thermal necrosis and shortest possible surgery time.

It is worth noting that, in addition to evaluating temperature, the role of the material removal rate (MRR) during the unloading process should also be considered. The faster the unloading process can be carried out, the more beneficial it is in terms of reducing surgery and anesthesia time, minimizing tissue damage, and shortening the patient's recovery period. Therefore, the material removal rate can be regarded as an influential factor alongside the thermal effects of the process. According to the results obtained from the optimization study, the parameters that lead to the minimum process temperature also correspond to the minimum material removal rate. Under these conditions, the theoretical material removal rate is 400 mm^3/min. However, to achieve the maximum material removal rate while considering necrosis prevention, optimal input parameters were identified as follows: tool diameter of 4 mm, feed rate of 100 mm/min, spindle speed of 1000 rpm and cutting depth of 1 mm. Under these conditions, the temperature reaches 54.4 °C, and the material removal rate is 2400 mm^3/min. These conditions, which simultaneously account for both temperature control and material removal efficiency, can be clinically effective and beneficial.

In orthopedic surgeries, the speed of surgery is very crucial, especially with the usage of assisting robots. This is highly influenced by feed rate and cutting depth. The results of this study provide meaningful guidance for surgical tool selection. Specifically, using tools with smaller diameters leads to lower temperatures during the milling process, thereby reducing the risk of thermal necrosis. From a clinical perspective, this implies that thinner tools not only improve thermal safety but also may contribute to shorter recovery times and reduced surgical complications. These insights support more informed decisions in selecting surgical parameters to balance efficiency and patient safety.

Table 5. Validity of the model for the optimum combination of parameters

T (°C)	D (mm)	Depth (mm)	F (mm/min)	N (rpm)	Optimization
42.58	4	1	100	1000	**Model**
42.3	4	1	100	1000	**Experiment**
0.28%	-	-	-	-	**Error percentage**

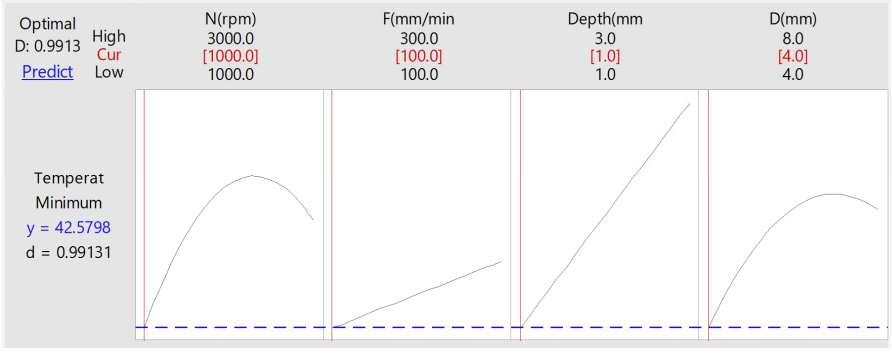

Fig. 12. Optimization of input parameters to achieve the minimum temperature.

6. Conclusions

This paper performed a systematic design of experiment, intelligent modeling, and sensitivity analysis of the bone grinding process using the XGBoost machine learning method and the Sobol approach. The input parameters tested were tool rotational speed, feed rate, cutting depth, and tool diameter, with process temperature being the output parameter. The primary findings of the current study are as follows:

- The XGBoost model continually showed strong performance in predicting the temperature of the milling process. During the training phase, the model demonstrated a noteworthy alignment between predicted and actual values as it gathered the data. This alignment was also evident in the testing phase, as the model's predictions closely corresponded with the actual data points. The assessment emphasized the model's accuracy in predicting temperature, focusing on the consistency between test data and the model's predictions as a key indicator of its reliability.
- The XGBoost model's performance was thoroughly evaluated utilizing key metrics including determination coefficient (R^2) and mean absolute percentage error (MAPE) throughout both training and testing phases. The R^2 values of 0.99 for the training phase and 0.94 for the testing phase demonstrate a high degree of accuracy in representing the fluctuation of the process temperature. The model's efficiency in reducing prediction errors across all study stages is highlighted by the low MAPE values of 0.33% for training and 3.38% testing, respectively.
- Process temperature is greatly impacted by rotational speed. The study reveals a crucial juncture where temperature patterns shift. Reduced rotational speeds decrease the likelihood of thermal damage by lowering process forces, while higher speeds result in lower temperatures due to easier chip removal and the bone's poorer thermal conductivity.
- The feed rate, comparable to the velocity of the heat source, is essential. Typically, higher feed rates result in increased bone temperature because of elevated process pressures and chip thickness. The study highlights the relationship between frictional forces and heat generation, showing that higher feed rates lead to higher temperatures within the specified range of input variables.
- Cutting depth and tool diameter are often overlooked but significantly affect the process temperature. Greater cutting depths raise process temperature by expanding contact surfaces and increasing pressures. Tool diameter significantly impacts temperature, with larger diameters leading to exponential temperature rises. Larger tool sizes result in a narrower safe zone for avoiding thermal necrosis, which impacts surgery recovery times.
- Sobol sensitivity analysis is an accurate technique, although it can be costly to use. The parameters that had the greatest significant impact on maximum process temperature were cutting depth, rotating speed, tool diameter, and feed rate, with effectiveness percentages of 46.7%, 36%, 13.2%, and 4.1% correspondingly.
- The model was optimized to achieve the minimum process temperature and desirability value. Validating experiments showed an accuracy of 0.28% in predicting temperature with the optimum combination of input parameters. The least maximum process temperature was found at 4 mm tool diameter, 100 mm/min feed rate, 1000 rpm rotational speed, and 1 mm cutting depth, achieving 42 °C.
- To achieve the Maximum material removal rate while considering necrosis prevention, the optimal input parameters were identified as follows: tool diameter of 4 mm, feed rate of 100 mm/min, spindle speed of 1000 rpm, and cutting depth of 1 mm. Under these conditions, the temperature reaches 54.4 °C, and the material removal rate is 2400 mm³/min.

Authors' contributions

Vahid Tahmasbi: Conceptualization, Methodology, Software, Validation, Project administration, Writing - Review & Editing

Mahdi Qasemi: Software, Investigation, Formal analysis,

Original Draft, Data Curation

Amir Hossein Rabiee: Software, Resources, Writing - Review & Editing, Supervision

Conflict of interest

The authors declare that they have no known competing financial interests or personal relationships that could have appeared to influence the work reported in this paper.

Data availability

The data that support the findings of this study are available on request from the corresponding author.

Funding

This research did not receive any specific grant from funding agencies in the public, commercial, or not-for profit sectors.

7. References

[1] Dahotre, N. B., & Joshi, S. (2016). *Machining of bone and hard tissues*. Springer. https://doi.org/10.1007/978-3-319-39158-8

[2] Schröter, L., Kaiser, F., Küppers, O., Stein, S., Krüger, B., Wohlfahrt, P., Geroneit, I., Stahlhut, P., Gbureck, U., & Ignatius, A. (2024). Improving bone defect healing using magnesium phosphate granules with tailored degradation characteristics. *Dental Materials, 40*(3), 508–519. https://doi.org/10.1016/j.dental.2023.12.019

[3] Guenther, D., Schmidl, S., Klatte, T. O., Widhalm, H. K., Omar, M., Krettek, C., Gehrke, T., Kendoff, D., & Haasper, C. (2015). Overweight and obesity in hip and knee arthroplasty: Evaluation of 6,078 cases. *World Journal of Orthopedics, 6*(1), 137–144. https://doi.org/10.5312/wjo.v6.i1.137

[4] Aliyu, A. A. A., Abdul Rani, A. M., Ginta, T. L., Prakash, C., Axinte, E., Razak, M. A., & Ali, S. (2017). A review of additive mixed electric discharge machining: Current status and future perspectives for surface modification of biomedical implants. *Advances in Materials Science and Engineering*, 8723239. https://doi.org/10.1155/2017/8723239

[5] Pezzotti, G., & Yamamoto, K. (2014). Artificial hip joints: The biomaterials challenge. *Journal of the Mechanical Behavior of Biomedical Materials, 31*, 3–20. https://doi.org/10.1016/j.jmbbm.2013.06.001

[6] Plaskos, C. (2002). Bone sawing and milling in computer-assisted total knee arthroplasty [Master's thesis, University of British Columbia]. https://doi.org/10.14288/1.0080992

[7] Rosen, J., Hannaford, B., & Satava, R. M. (2011). *Surgical robotics: Systems applications and visions*. Springer Science & Business Media.

[8] Hernandez Montero, E., Caballero, E., & García Ibanez, L. (2020). Surgical management of middle cranial fossa bone defects: Meningoencephalic herniation and cerebrospinal fluid leaks. *American Journal of Otolaryngology*, *41*, 102560. https://doi.org/10.1016/j.amjoto.2020.102560

[9] Dahibhate, R. V., & Jaju, S. B. (2019). Bone drilling parameters and necrosis: An in vitro study. In *Smart Technologies for Energy, Environment and Sustainable Development: Select Proceedings of ICSTEESD 2018* (pp. 599–606). Singapore: Springer Singapore.

[10] Gallo, J., Goodman, S. B., Konttinen, Y. T., Wimmer, M. A., & Holinka, M. (2013). Osteolysis around total knee arthroplasty: A review of pathogenetic mechanisms. *Acta Biomaterialia, 9*, 8046–8058. https://doi.org/10.1016/j.actbio.2013.06.032

[11] Zhang, Y., Robles Linares, J. A., Chen, L., Liao, Z., Shih, A. J., & Wang, C. (2022). Advances in machining of hard tissues – from material removal mechanisms to tooling solutions. *International Journal of Machine Tools and Manufacture, 172*, 103838. https://doi.org/10.1016/j.ijmachtools.2021.103838

[12] Eriksson, A., & Albrektsson, T. (1983). Temperature threshold levels for heat induced bone tissue injury: A vital microscopic study in the rabbit. *The Journal of Prosthetic Dentistry*, *50*(1), 101–107. https://doi.org/10.1016/0022-3913(83)90174-9

[13] Berman, A. T., Spence, R. J., Yanicko, D. R., Sih, G. C., & Zimmerman, M. (1984). Thermally induced bone necrosis in rabbits: Relation to implant failure in humans. *Clinical Orthopaedics and Related Research*, *186*, 284–292. https://doi.org/10.3109/02844318409052849

[14] Lundskog, J. (1972). An experimental investigation of the thermal properties of bone tissue and threshold levels for thermal injury. *Scandinavian Journal of Plastic and Reconstructive Surgery*, *9*, 1–80.

[15] Bonfield, W., & Li, C. (1968). The temperature dependence of the deformation of bone. *Journal of Biomechanics*, *1*, 323–329. https://doi.org/10.1016/0021-9290(68)90026-2

[16] Eriksson, R., Albrektsson, T., & Magnusson, B. (1984). Assessment of bone viability after heat trauma: A histological, histochemical and vital microscopic study in the rabbit. *Scandinavian Journal of Plastic and Reconstructive Surgery*, *18*(3), 261–268. https://doi.org/10.3109/02844318409052849

[17] Eriksson, R., & Albrektsson, T. (1984). The effect of heat on bone regeneration: An experimental study in the rabbit using the bone growth chamber. *Journal of Oral*

and Maxillofacial Surgery, *42*, 705–711. https://doi.org/10.1016/0278-2391(84)90417-8

[18] Eriksson, R. A., & Adell, R. (1986). Temperatures during drilling for the placement of implants using the osseointegration technique. *Journal of Oral and Maxillofacial Surgery*, *44*, 4–7. https://doi.org/10.1001/joms.1986.00860030056014

[19] Al Abdullah, K. I. A. L., Abdi, H., Lim, C. P., & Yassin, W. A. (2018). Force and temperature modelling of bone milling using artificial neural networks. *Measurement, 116*, 25–37. https://doi.org/10.1016/j.measurement.2017.10.051

[20] Liao, Z., Axinte, D., & Gao, D. (2019). On modelling of cutting force and temperature in bone milling. *Journal of Materials Processing Technology, 266*, 627–638. https://doi.org/10.1016/j.jmatprotec.2018.11.039

[21] Tahmasbi, V., Ghoreishi, M., & Zolfaghari, M. (2017). Investigation, sensitivity analysis, and multi-objective optimization of effective parameters on temperature and force in robotic drilling cortical bone. *Proceedings of the Institution of Mechanical Engineers, Part H: Journal of Engineering in Medicine, 231*(11), 1012–1024. https://doi.org/10.1177/0954411917726098

[22] Hassanalideh, H. H., & Gholampour, S. (2020). Finding the optimal drill bit material and proper drilling condition for utilization in the programming of robot-assisted drilling of bone. *CIRP Journal of Manufacturing Science and Technology, 31*, 34–47. https://doi.org/10.1016/j.cirpj.2020.09.011

[23] Shin, H., & Yoon, Y.-S. (2006). Bone temperature estimation during orthopaedic round bur milling operations. *Journal of Biomechanics, 39*, 33–39.

[24] Sugita, N., Osa, T., & Mitsuishi, M. (2009). Analysis and estimation of cutting-temperature distribution during end milling in relation to orthopedic surgery. *Medical Engineering & Physics, 31*, 101–107. https://doi.org/10.1016/j.medengphy.2008.05.005

[25] Malvisi, A., Vendruscolo, P., Morici, F., Martelli, S., & Marcacci, M. (2000). Milling versus sawing: Comparison of temperature elevation and clinical performance during bone cutting. In *International Conference on Medical Image Computing and Computer-Assisted Intervention* (pp. 1238–1244). Berlin, Heidelberg: Springer Berlin Heidelberg.

[26] Talebi Ghadikolaee, H., Moslemi Naeini, H., Rabiee, A. H., Zeinolabedin Beygi, A., & Alexandrov, S. (2023). Experimental numerical analysis of ductile damage modeling of aluminum alloy using a hybrid approach: Ductile fracture criteria and adaptive neural fuzzy system (ANFIS). *International Journal of Modelling and Simulation, 43*(4), 736–751. https://doi.org/10.1080/02286203.2023.11866137

[27] Rabiee, A. H., Sherkatghanad, E., Zeinolabedin Beygi, A., Moslemi Naeini, H., & Lang, L. (2023). Experimental investigation and modeling of fiber metal laminates hydroforming process by GWO optimized neuro fuzzy network. *Journal of Computational & Applied Research in Mechanical Engineering (JCARME), 12*, 193–209. https://doi.org/10.22059/jcarme.2023.342589.623

[28] Safari, M., Rabiee, A., & Tahmasbi, V. (2022). Resistance spot welding process of AISI 304 steel: Application of sensitivity analysis and ANFIS GWO methods. *Journal of Stress Analysis, 6*, 21–29. https://doi.org/10.22059/jsa.2022.337368.1060

[29] Liu, C., He, Y., Li, Y., Wang, Y., Wang, L., Wang, S., & Wang, Y. (2021). Predicting residual properties of ball screw raceway in whirling milling based on machine learning. *Measurement, 173*, 108605. https://doi.org/10.1016/j.measurement.2020.108605

[30] Du, C., Ho, C. L., & Kaminski, J. (2021). Prediction of product roughness, profile, and roundness using machine learning techniques for a hard turning process. *Advances in Manufacturing, 9*, 206–215. https://doi.org/10.1007/s40436-021-00385-y

[31] He, Z., Shi, T., Xuan, J., & Li, T. (2021). Research on tool wear prediction based on temperature signals and deep learning. *Wear*, 478–479, 203902. https://doi.org/10.1016/j.wear.2021.203902

[32] Varghese, A., Kulkarni, V., & Joshi, S. S. (2021). Tool life stage prediction in micro milling from force signal analysis using machine learning methods. *Journal of Manufacturing Science and Engineering, 143*(5), 054501. https://doi.org/10.1115/1.4048636

[33] Tahmasbi, V., & Rabiee, A. H. (2022). Intelligent temperature modeling in robotic cortical bone milling process based on teaching learning-based optimization algorithm. *Proceedings of the Institution of Mechanical Engineers, Part H: Journal of Engineering in Medicine, 236*(8), 1118–1128. https://doi.org/10.1177/09544119221106822

[34] Safari, M., Tahmasbi, V., & Rabiee, A. H. (2021). Investigation into the automatic drilling of cortical bones using ANFIS-PSO and sensitivity analysis. *Neural Computing and Applications, 33*(23), 16499–16517. https://doi.org/10.1007/s00521-021-06248-4

[35] Banda, T., Liu, Y.-C., Farid, A. A., & Lim, C. S. (2023). A machine learning model for flank wear prediction in face milling of Inconel 718. *The International Journal of Advanced Manufacturing Technology, 126*(7–8), 935–945. https://doi.org/10.1007/s00170-023-11152-3

[36] Rabiee, A. H., Tahmasbi, V., & Qasemi, M. (2023). Experimental evaluation, modeling and sensitivity analysis of temperature and cutting force in bone micro milling using support vector regression and EFAST

methods. *Engineering Applications of Artificial Intelligence, 120*, 105874. https://doi.org/10.1016/j.engappai.2023.105874

[37] Zeng, S., & Pi, D. (2023). Milling surface roughness prediction based on physics informed machine learning. *Sensors, 23*, 4969. https://doi.org/10.3390/s23094969

[38] Araghizad, A. E., Pashmforoush, F., Tehranizadeh, F., Kilic, K., & Budak, E. (2024). Improving milling force predictions: A hybrid approach integrating physics based simulation and machine learning for remarkable accuracy across diverse unseen materials and tool types. *Journal of Manufacturing Processes, 114*, 92–107. https://doi.org/10.1016/j.jmapro.2024.02.015

[39] Chen, T., & Guestrin, C. (2016). XGBoost: A scalable tree boosting system. In *Proceedings of the 22nd ACM SIGKDD International Conference on Knowledge Discovery and Data Mining* (pp. 785–794). https://doi.org/10.1145/2939672.2939785

[40] Asselman, A., Khaldi, M., & Aammou, S. (2023). Enhancing the prediction of student performance based on the machine learning XGBoost algorithm. *Interactive Learning Environments, 31*(6), 3360–3379. https://doi.org/10.1080/10494820.2021.1928235

[41] Wang, C.-C., Kuo, P.-H., & Chen, G.-Y. (2022). Machine learning prediction of turning precision using optimized XGBoost model. *Applied Sciences, 12*(15), 7739. https://doi.org/10.3390/app12157739

[42] Zhang, X. Y., Trame, M. N., Lesko, L. J., & Schmidt, S. (2015). Sobol sensitivity analysis: A tool to guide the development and evaluation of systems pharmacology models. *CPT: Pharmacometrics & Systems Pharmacology, 4*(2), 69–79. https://doi.org/10.1002/psp4.6

[43] Nossent, J., Elsen, P., & Bauwens, W. (2011). Sobol's sensitivity analysis of a complex environmental model. *Environmental Modelling & Software, 26*, 1515–1525. https://doi.org/10.1016/j.envsoft.2011.06.019

[44] Kumar, D., Singh, A., Kumar, P., Jha, R. K., Sahoo, S. K., & Jha, V. (2020). Sobol sensitivity analysis for risk assessment of uranium in groundwater. *Environmental Geochemistry and Health*, *42*, 1789–1801. https://doi.org/10.1007/s10653-020-00522-5